MASS AND MOMENTUM TRANSPORT EXPERIMENTS WITH SWIRLING FLOW

Bruce V. Johnson and Richard Roback
United Technologies Research Center

An experimental study of mixing downstream of axial and swirling coaxial jets is being conducted to obtain data for the evaluation and improvement of turbulent transport models currently employed in a variety of computational procedures used throughout the propulsion community. The axial coaxial jet study was completed under Phase I and is reported in Ref. 1. The swirling coaxial jet study, which is the subject of this paper, was conducted under Phase II of the contract and is reported in Ref. 2. A TEACH code was acquired, checked out for several test cases, and is reported in Ref. 3. A study to measure length scales and to obtain a limited number of measurements with a blunt trailing edge inlet is being conducted under Phase III of the contract.

Qualitative and quantitative studies were conducted of the flow downstream of swirling coaxial jets discharging into an expanded duct. The ratio of annular jet diameter and duct diameter to the inner jet diameter were approximately 2 and 4, respectively. The inner jet peak axial velocity was approximately one-half the annular jet peak axial velocity and the mean swirl angle in the annular stream was approximately 30 degrees. Results from the studies were related to the five shear regions within the duct: (1) the wake region downstream of the inlet, (2) the shear layer between the jets, (3) the annular recirculation region, (4) the reattachment region, and (5) the centerline recirculation region (Fig. 1).

A flow visualization study was conducted using fluorescence dye as a trace material and high-speed motion pictures to record the dye patterns in selected r-z and r-θ planes. The results of the flow visualization study are summarized with the following observations (Figs. 2 and 3):

1. The high intensity turbulent eddies in the shear layers were not axisymmetric or periodic. The large scale waves and eddies apeared to have a range of wavelengths.

2. Downstream of the centerline recirculation region, the flow initially had large lobes which evolved into a vortex swirl pattern. There was little radial mixing downstream of the recirculation cell.

3. Two major mixing regions were observed: (1) at the interface between the inner jet and the centerline recirculation zone, and (2) at the interface between the inner jet and annular jet streams.

4. Mixing at the interface of the inner stream and the recirculation cell diluted the inner jet concentration and the resulting mixture of fluid from the recirculation cell and the inner jet was entrained by the swirling annular stream.

A detailed map of the velocity, concentration , mass turbulent transport rate and momentum turbulent transport rate distributions within the test section was obtained to provide data for the evaluation and improvement of turbulent transport models. Data sets of velocity component pairs were obtained simultaneously to determine mass turbulent transport rate, concentration and velocity. Probability density

functions (p.d.f.s) of all the forementioned parameters were obtained from the data sets. Mean quantitites (Figs. 4, 6 and 7), second central moments (Fig. 5), correlation coefficients, skewness and kurtosis were calculated to characterize each data set. Following are the principal results from this study:

1. Mixing for swirling flow was completed in one-third the length required for nonswirling flows (Figs. 8 and 9).

2. The principal momentum turbulent transport was in the r-z plane, i.e. $\overline{uv}$, and was attributed to the axial velocity gradients. Peak momentum turbulent transport rates were approximately the same as for the nonswirling flow condition (Fig. 6).

3. The axial mass turbulent transport is gradient rather than countergradient as occurred for nonswirling flow. The peak axial mass transport rates were greater than the peak radial mass transport rates even though the axial concentration gradients were approximately one-seventh the radial gradients (Figs. 4 and 7).

4. The mass turbulent transport process for swirling coaxial flow is very complicated. Mixing appears to occur in several steps of axial and radial mass transport coupled with a large radial mean convective flux. The transport process appears to begin with high concentration fluid from the inner jet mixing with fluid from the centerline recirculation zone. The diluted inner jet fluid is then convected by the negative axial velocities into the large eddy shear region between inner and annular streams.

5. Axial mass turbulent transport correlation coefficients as high as 0.5 were measured. These correlation coefficients were less than the peak mass transport correlation coefficients obtained for nonswirling flow although the axial mass transport rate for swirling flow was greater than that for nonswirling flow.

References

1. Johnson, B. V. and J. C. Bennett: Mass and Momentum Turbulent Transport Experiments with Confined Coaxial Jets, NASA Contractor Report CR-165574 (Interim Summary Report), November 1981.

2. Roback, R. and B. V. Johnson: Mass and Momentum Turbulent Transport Experiments with Confined Swirling Coaxial Jets, NASA Contractor Report CR-168252 (Interim Summary Report), August 1983.

3. Chiappetta, L. M.: User's Manual for a TEACH Computer Program for the Analysis of Turbulent, Swirling Reacting Flow in a Research Combustor. UTRC Report R83-915540-27 prepared under NASA Contract NAS3-22771, September 1983.

FIG. 1

SHEAR REGIONS WITH CONFINED, EXPANDING COAXIAL JETS

a) SWIRLING FLOW

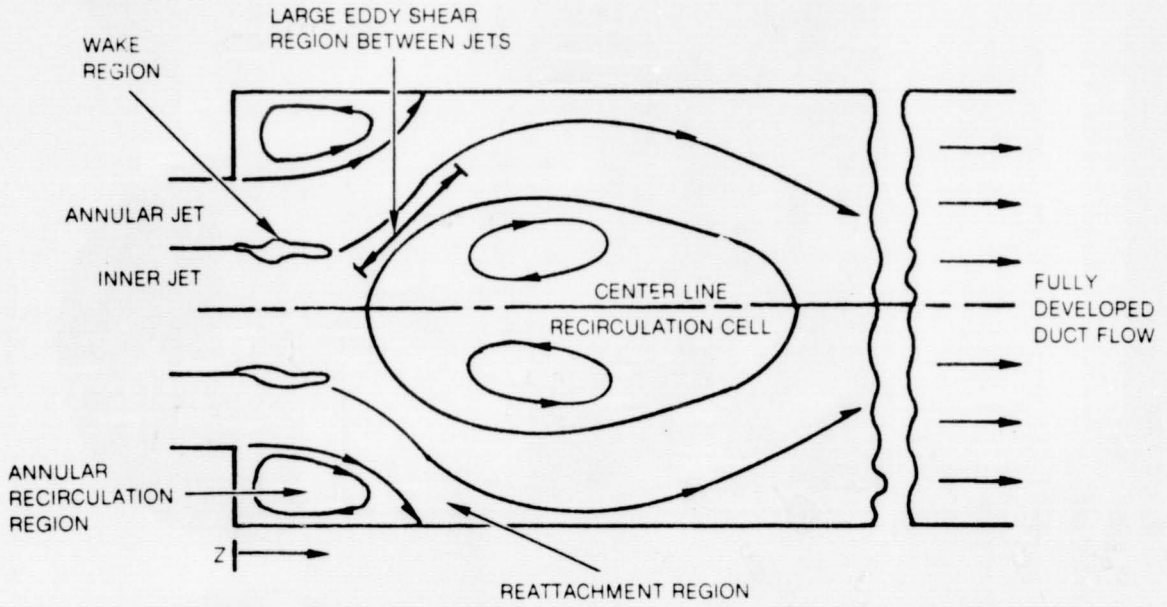

b) NONSWIRLING FLOW

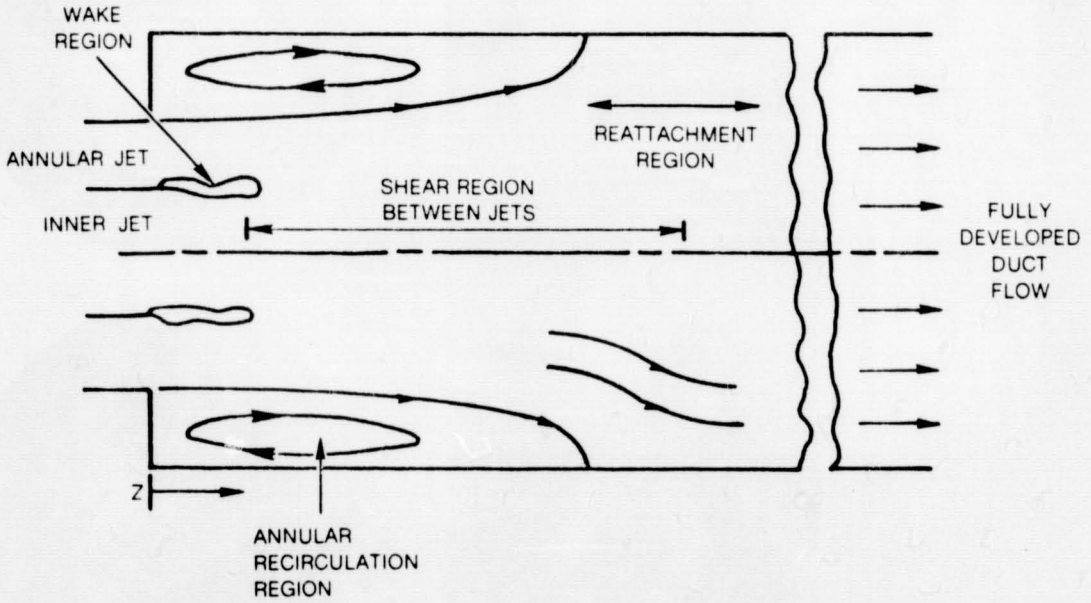

VISUALIZATION OF FLOW

$U_i = 0.52$ m/s $\quad U_a = 1.66$ m/s

$Q_i = 6.2$ gpm $\quad Q_a = 52.8$ gpm

r-z PLANE

$0 < z < 230$ mm

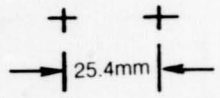

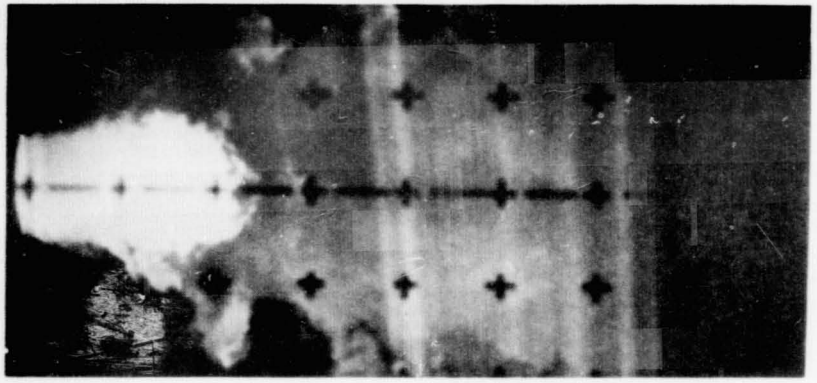

DYE ADDED TO INNER STREAM

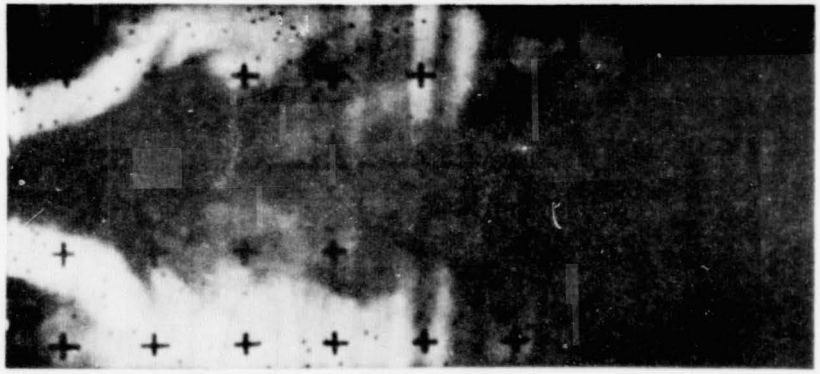

DYE ADDED TO ANNULAR STREAM

r-θ PLANE

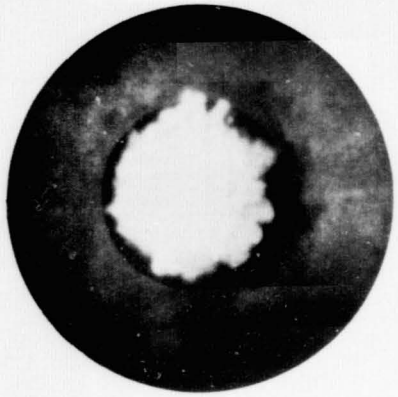

$z = 25$ mm

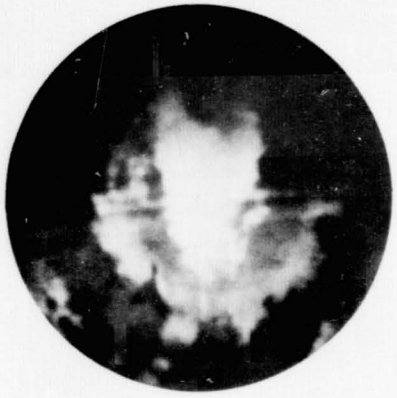

$z = 51$ mm

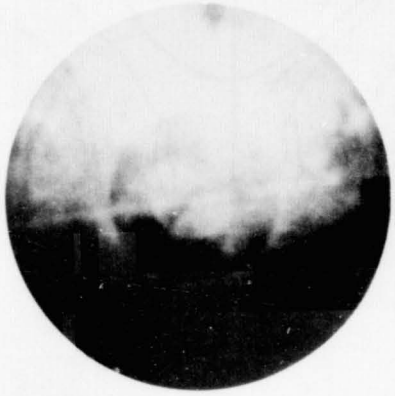

$z = 102$ mm

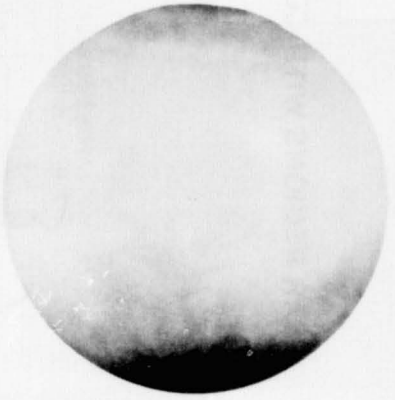

$z = 203$ mm

DYE ADDED TO INNER STREAM

FIG. 2

FIG. 3

VISUALIZATION OF FLOW

$U_i = 0.52$ m/s $U_a = 1.66$ m/s

$Q_i = 6.2$ gpm $Q_a = 52.8$ gpm

DYE ADDED TO ANNULAR STREAM

r-θ PLANE

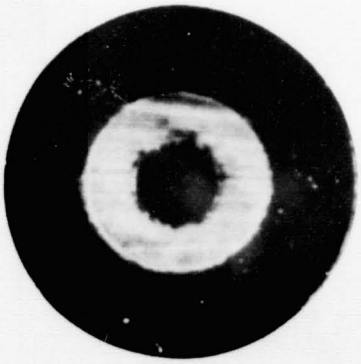

z = 5 mm

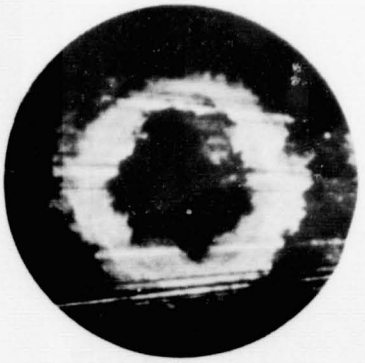

z = 25 mm

z = 38 mm

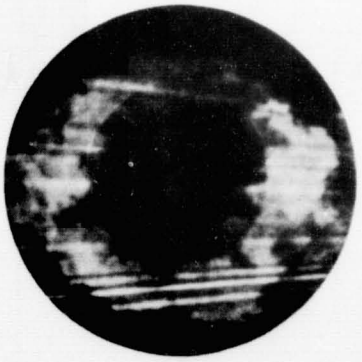

z = 51 mm

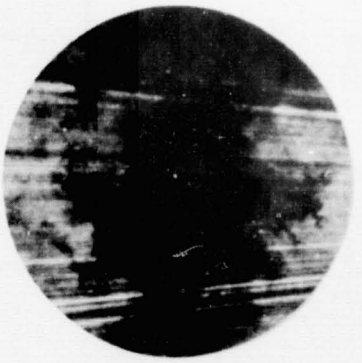

z = 102 mm

z = 152 mm

z = 203 mm

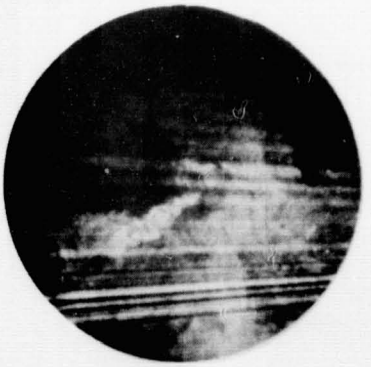

z = 305 mm

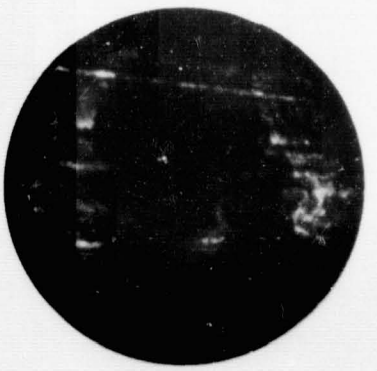

z = 406 mm

FIG. 4

MEAN VELOCITY AND INNER JET CONCENTRATION PROFILES AT z = 25 mm

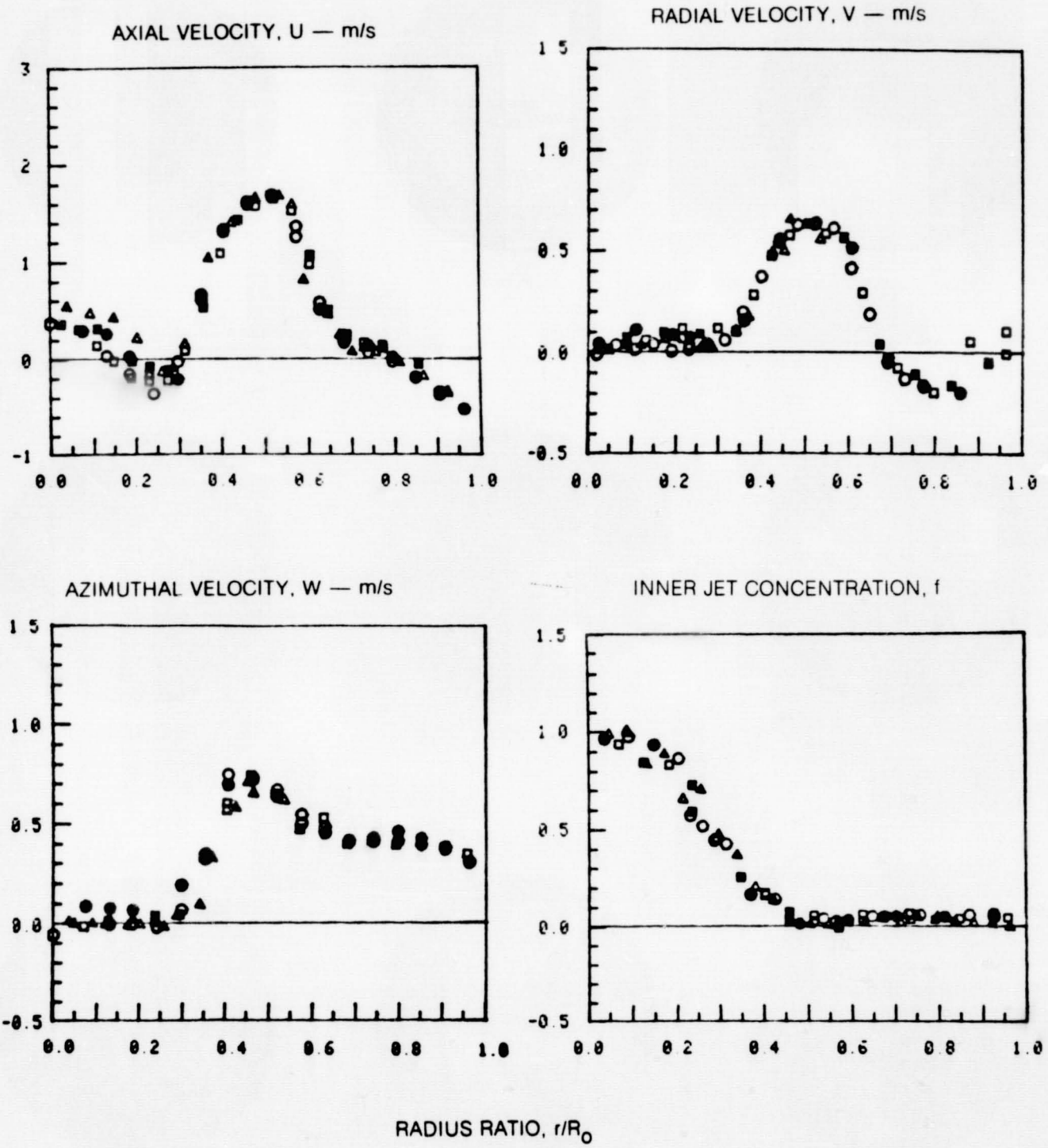

FIG. 5

FLUCTUATING VELOCITY AND INNER JET CONCENTRATION PROFILES AT z = 25 mm

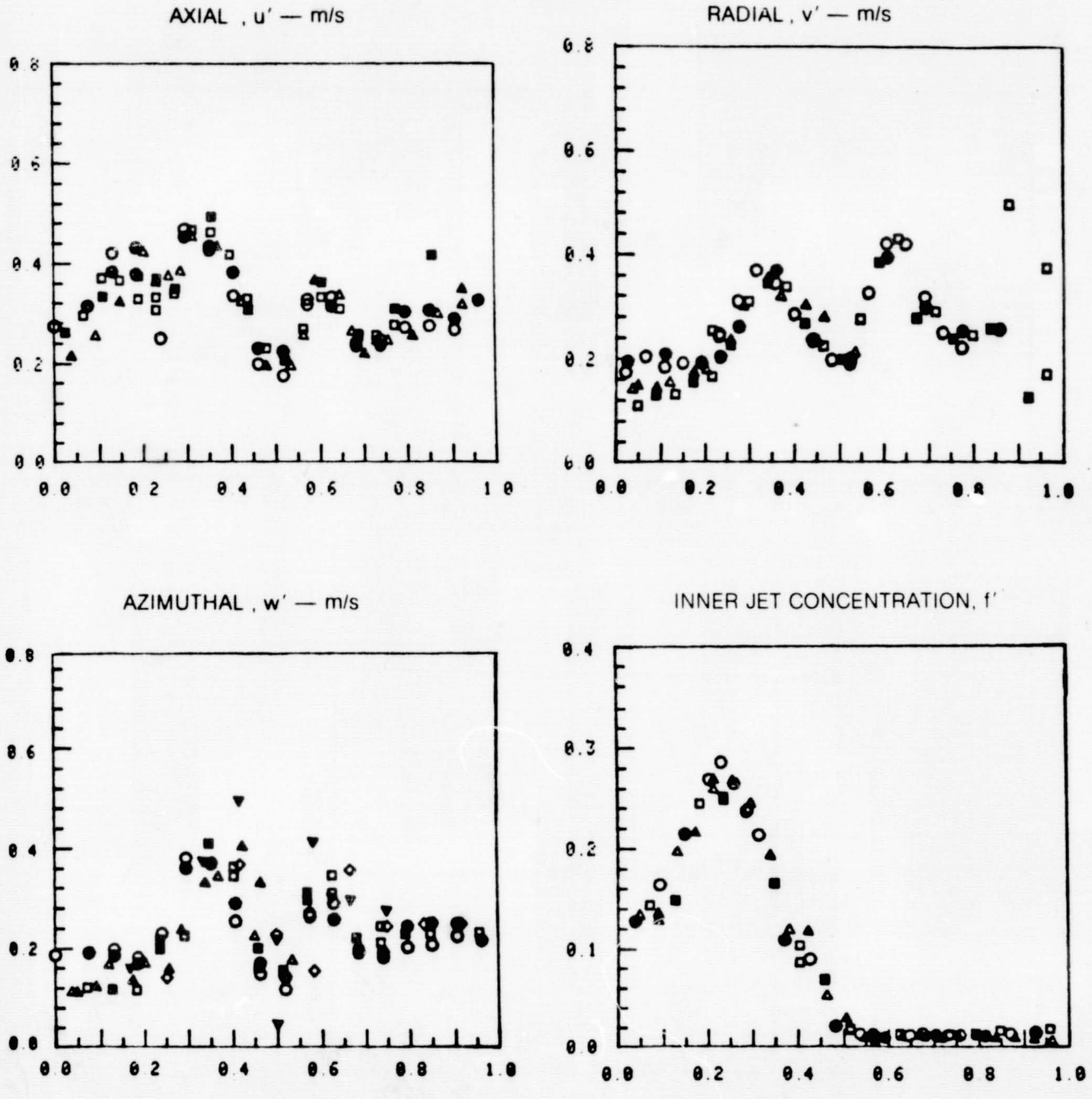

FIG. 6

MOMENTUM TURBULENT TRANSPORT RATE PROFILES AT z = 25 mm

r-z PLANE, $\overline{uv}$ — m^2s^2

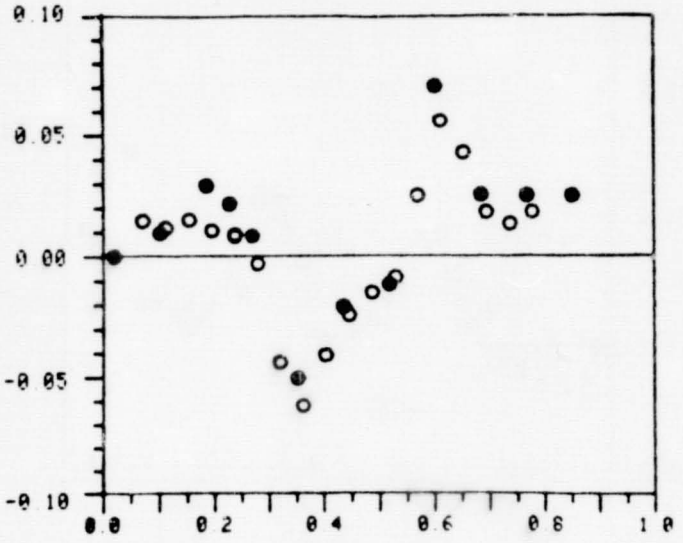

θ-z PLANE, $\overline{uw}$ — m^2/s^2

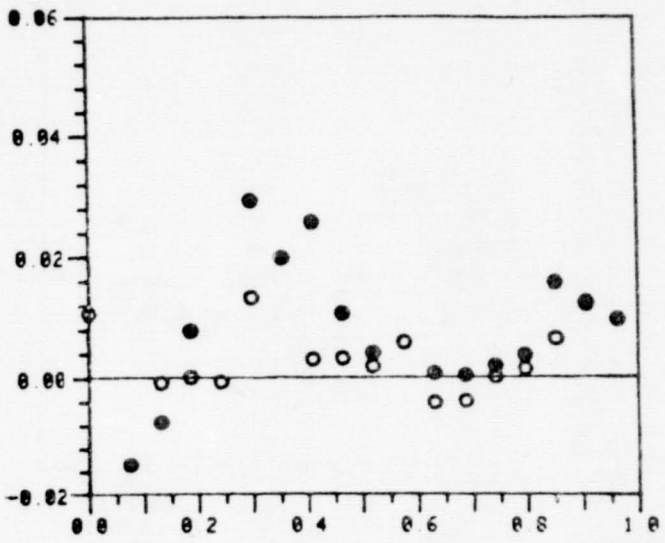

r-θ, PLANE, $\overline{wv}$ — m^2s^2

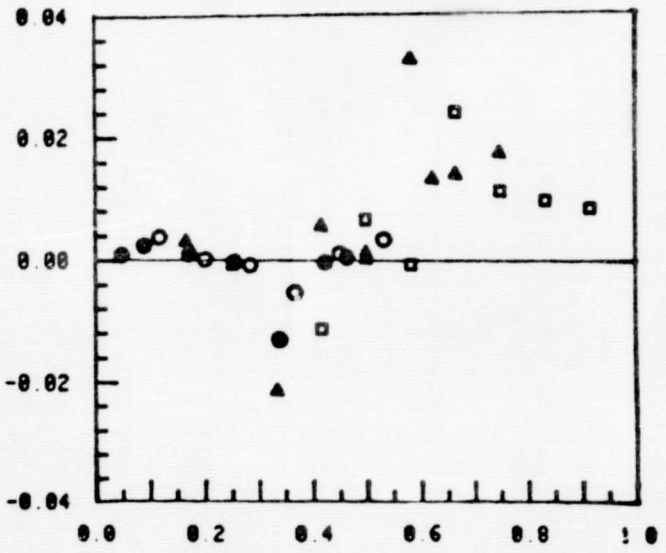

RADIUS RATIO, r/R_o

FIG. 7

MASS TURBULENT TRANSPORT RATE PROFILES AT z = 25 mm

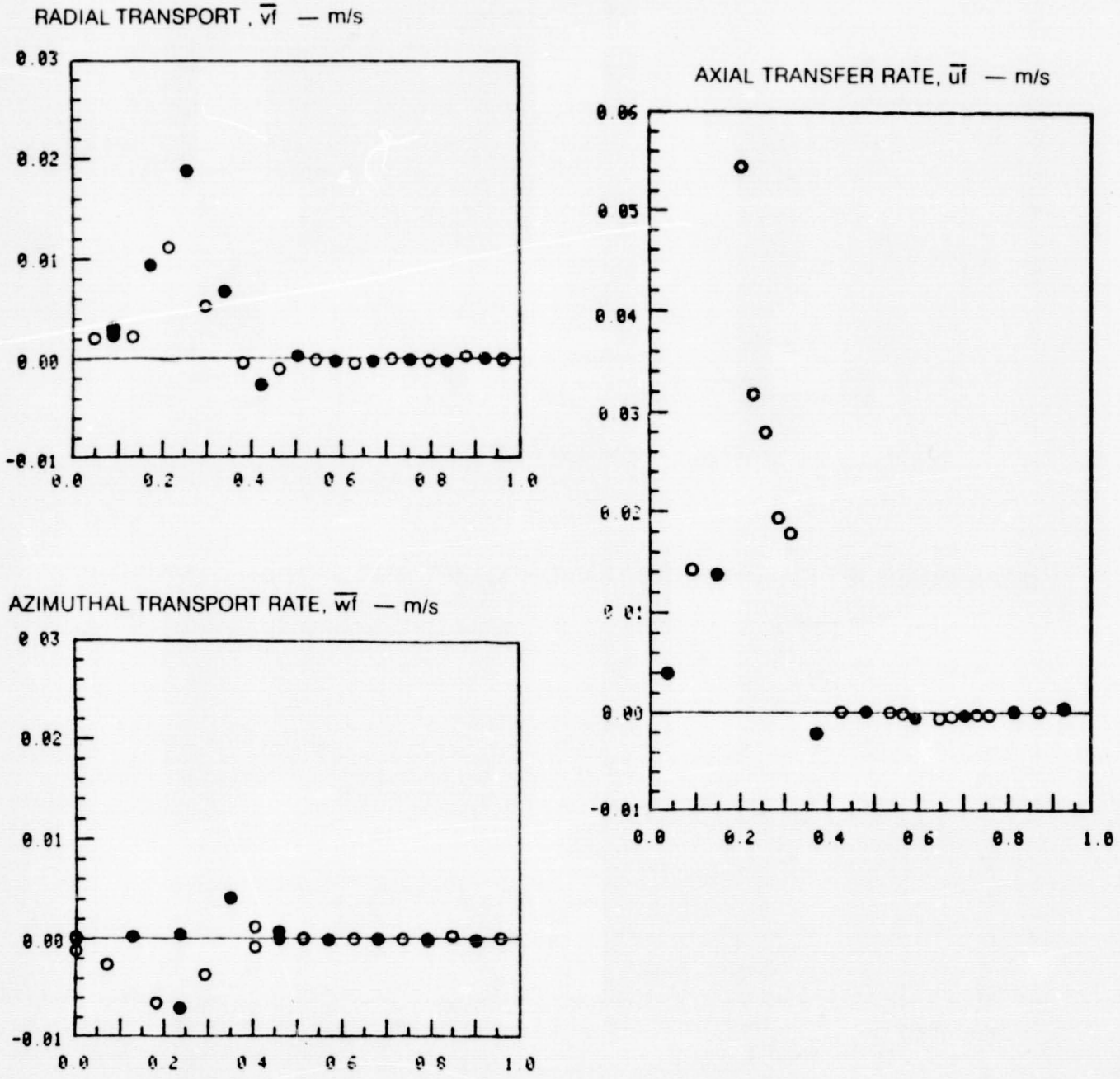

FIG. 8

MEAN AXIAL VELOCITY ALONG TEST SECTION CENTERLINE

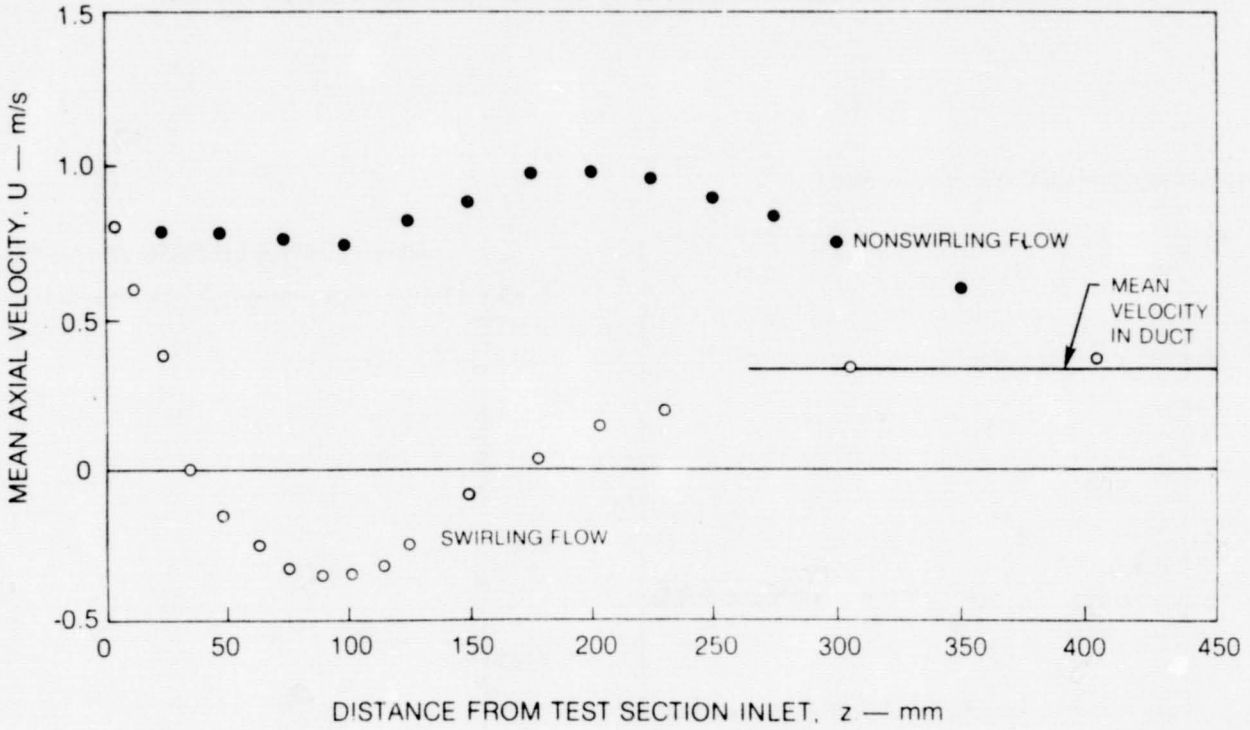

FIG. 9

MEAN INNER JET FLUID CONCENTRATION ALONG TEST SECTION CENTERLINE